# PV MODULE PERFORMANCE MEASUREMENTS – STATISTICAL ANALYSIS OF TECHNOLOGICAL TRENDS

Ulli Kräling[1], Paul Gebhardt[1], Martin Kaiser[1], Daniel Philipp[1]
[1]Fraunhofer Institute for Solar Energy Systems
Heidenhofstr. 2, 79110 Freiburg, Germany

ABSTRACT: Determining the performance of photovoltaic (PV) modules accurately and in different operational states is key for evaluating their value and basic requirements for yield assessments and bankability considerations. In this publication, we share our experience from the last 10 years of performance measurements and module calibrations at the CalLab PV Modules of Fraunhofer ISE. Our dataset of STC results comprises 61060 modules from 739 different manufacturers (3548 different module types) from North America, Europe, and Asia. We thereby present a valuable reference for various stakeholders in the PV community summarizing changes in performance and efficiency over time. Furthermore, we present and discuss technology trends, including the effect of module design aspects such as number of ribbons, wafer size, number of cells and cell technology on the performance at standard conditions, module parameters such as temperature coefficient and low light performance.
Keywords: PV module, efficiency, low light behavior, temperature coefficient, technology trends

## 1 INTRODUCTION

Determining the performance of photovoltaic (PV) modules accurately and in different operational states is a key quality indicator and a basic requirement for yield assessments and bankability considerations. These measurements are carried out according to standards IEC 60904-1 [1], IEC 60891 [2], and IEC 61853-1 [3]. At CalLab PV Modules, located at the Fraunhofer Institute for Solar Energy Systems ISE in Freiburg, Germany, we have carried out these measurements on a large scale for more than a decade for different purposes like calibration and quality control.

Here, we present performance data of a large set of PV modules from the last 10 years, as measured according to international standards IEC 60904-1 [1], IEC 60891 [2], and IEC 61853-1 [3]. This data could potentially serve as reference when evaluating or modelling the effect of different module technologies, or help estimating the effect on the energy rating or energy yield, since the discussed data is typically the input data for energy rating calculations.

The given data and analyses can serve as reference for different stakeholders of the PV community: Researchers can use it as indication of performance and weak light behavior for current and past modules, e.g., for theoretical considerations. Likewise, the presented data can be used to validate modelled/projected technology improvements [4].

## 2 METHODOLOGY

Fraunhofer ISE's accredited laboratory CalLab PV Modules produces measurement results for its customers with highest accuracy since more than a decade [5]. Beside the measurement results, basic characteristics of each module, e.g., manufacturer, module type, module dimensions, and cell material are recorded. More details were added in the recent years (e.g., number of cells, cell dimensions, and ribbons). So, for recent measurements, more module characteristics are available than for measurements 5 years ago.

All these results are used in an anonymized way to analyze the development of the discussed module characteristics in the past ten years.

### 2.1 Initial data set

The evaluation of the data is based on the period 2011/12 – 2022/08. Within this period, all measurement results were evaluated using the same inhouse developed software.

Different types of measurements are considered in this analysis: Measurement at Standard Test Conditions (25 °C, 1000 W/m²) according to IEC 60904-1 [1]; measurement at 25 °C and varying irradiance levels from 100 W/m² to 1100 W/m² according to IEC 60904-1 [1] and IEC 61853-1 [3]; measurement of temperature coefficients at 1000 W/m² according to IEC 60891 [2] and IEC 61853-1 [3]. Measurement types and conditions and the used abbreviations are shown in Table I.

**Table I:** Measurement types, abbreviations, and measurement conditions

| Measurement type | abbr. | Temperture [°C] | Irradiance [W/m²] |
|---|---|---|---|
| Standard test condition | STC | 25 | 1000 |
| Irradiance dependency | G | 25 | 100 - 1100 |
| Temperature coefficient | TC | 15 - 75 | 1000 |

The measured modules considered in this analysis are property of Fraunhofer ISE's customers and belong to different types of projects with different objectives. This includes large sets of identical modules of the same type, e.g., from a PV power plant or single modules, e.g., golden modules in a production line. Beside the number of modules per type (i.e. product name), also the number of measurements for an individual module varies because the evaluation of light-induced degradation (LID), light- and elevated temperature-induced degradation (LETID) [6], potential-induced degradation (PID), and others, requires module measurements at different states of degradation.

To make measurement results comparable, several filters were applied. Thus, only measurements of the same state are extracted and the imbalance between large and small groups of identical measurement objects is eliminated. So, the final data set still represents the variety of all modules measured at Fraunhofer ISE's module calibration lab CalLab PV Modules. The filtering steps are described in detail in the following section.

2.2 Inconsistency filter

The initial filter sorts out measurement results with inconsistent data. E.g., target temperature and target irradiance must align with the designated measurement type. The serial number of the device under test (DUT) in the results information is mandatory to identify repeating measurements. Measurements of the rear side of bifacial modules are also excluded. Finally, data sets with physically impossible results are excluded, like negative short circuit current $I_{SC}$, negative open circuit voltage $V_{OC}$ or fill factor beyond 100 %. Those results might come from measurements of defective modules (e.g., due to transportation damage).

2.3 Initial measurement filter

The 2nd filter only preserves the first measurement – of a specific measurement type like STC – of a DUT within a project. The intention is to get only results at initial state of the module. This is the only comparable state over a large set of data because the intermediate state of a module depends on the individual schedule and focus of a project and therefore differs for each project. This also means that the herein presented data was acquired before any stabilization, e. g. by light soaking.

2.4 First appearance filter

The 3rd filter removes data sets of recalibrations and other re-measurements. Typically, golden modules are sent to our lab to be recalibrated in regular time intervals. Then, the identical module refers to different projects respectively orders. To avoid double counting of these modules, only the first appearance of a serial number of a specific module is valid and all subsequent remeasurements of a module are sorted out.

2.5 Imbalance filter

In the next step, from each module type in a project, only the measurement results closest to the average power (respectively the average $TC_{Pmpp}$ for TC measurements) for this module type is considered. Hence, the imbalance due to different numbers of modules per project is eliminated. In addition, this paper is focused on general and representative trends in PV module development and not in the presentation of highest possible results.

## 3 RESULTS AND DISCUSSION

3.1 Filter characteristics

61060 STC measurements, 1382 irradiance dependence measurements (G) and 1381 temperature coefficient measurements (TC) in the period 2011/12 – 2022/08 were analyzed. By different filtering algorithms described in the previous section, data sets were significantly reduced to 9.7 % for STC, 40.9 % for G and 58.1 % for TC measurements compared to the initial available data sets. The available data sets after the individual filtering steps are shown in Table II.

**Table II:** Number of available data sets after several filtering steps for STC, irradiance dependence (G) and temperature coefficients (TC) measurements and ratio of filtered data.

| Filter steps | STC | G | TC |
|---|---|---|---|
| 0 Initial data set | 61060 | 1382 | 1381 |
| 1 Inconsistency filter | 58282 | 1243 | 1320 |
| 2 Initial measurements | 37066 | 979 | 1217 |
| 3 First appearance filter | 36357 | 964 | 1204 |
| 4 Imbalance filter | 5940 | 565 | 803 |
| Ratio (filtered/initial) | 9.7 % | 40.9 % | 58.1 % |

The filtering was also analyzed for mono-Si and poly-Si modules separately (Table III). The filter ratio for mono-Si and poly-Si modules was nearly identical for STC. For G and TC, the ratio for mono-Si was about 5 % points lower than for poly-Si.

**Table III:** Filtering results for mono-Si and poly-Si modules for different measurement types.

| Standard test conditions (STC) | poly-Si | mono-Si |
|---|---|---|
| Available | 26848 | 28155 |
| Filtered | 2618 | 2740 |
| Ratio | 9.8 % | 9.7 % |

| Irrandiance dependency (G) | poly-Si | mono-Si |
|---|---|---|
| Available | 544 | 682 |
| Filtered | 243 | 271 |
| Ratio | 44.7 % | 39.7 % |

| Temperature coefficient (TC) | poly-Si | mono-Si |
|---|---|---|
| Available | 612 | 652 |
| Filtered | 377 | 371 |
| Ratio | 61.6 % | 56.9 % |

In Figure 1, the filtering of the data is shown for STC results for mono-Si modules. The different color grades indicate the different intermediate filtering steps, from initial data set (light gray) to filtered data (dark blue). After filtering, a clear trend over the years towards higher efficiencies is already visible as will be discussed in detail later.

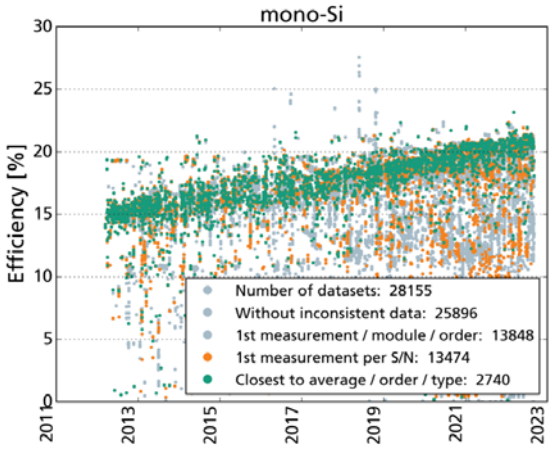


**Figure 1:** Visualization of data filtering for mono-Si PV modules. Measured efficiencies at STC are shown vs.

measurement date. The different colors indicate the different filtering levels.

As indicated in Table II, filtering reduced the number of data sets, e.g., for STC to 9.7 % of the initial data sets. Nevertheless, more than 92 % of module types and producers are still available in the filtered data sets as shown in Table IV. Hence, the diversity of producers and modules could be preserved after filtering and the imbalance of different sample sizes and re-measurements was eliminated. 686 different PV module producers and 3508 different PV module types remain after filtering for evaluation. The inconsistency filter causes the reduction of producers and module types in the data set.

**Table IV:** Available number of producers and module types in the data sets before and after filtering for different measurement types

| Producers | STC | G | TC |
|---|---|---|---|
| Available | 739 | 156 | 194 |
| Filtered | 686 | 145 | 187 |
| Ratio | 92.8 % | 92.9 % | 96.4 % |

| Module types | STC | G | TK |
|---|---|---|---|
| Available | 3548 | 511 | 693 |
| Filtered | 3508 | 479 | 687 |
| Ratio | 98.9 % | 93.7 % | 99.1 % |

3.2 Technology trends

Beside the measurement results, the documented module characteristics give an overview of the technological development over the past 10 years. As an independent accredited calibration and testing lab, CalLab PV Modules is not involved in the module development and has therefore only limited access to detailed information about the module components and related technologies. Therefore, the analysis is mainly focused on visible characteristics and information stated on the module label or datasheet values provided by the customer. The presented results in this section are based on the filtered STC results.

The number of ribbons per cell was monitored from 2016 on. Figure 2 shows the share of different ribbon numbers for each year. Until 2020, modules with 5 or less ribbons were dominating for mono-Si modules with a share of more than 50 %. Since then, the share drastically dropped and modules with 9 or 10 thinner ribbons or round wires took over the lead [7].

For poly-Si modules, the 5-ribbon technology is still dominating. The reason for this difference to mono-Si modules could be the lack of process development for poly-Si modules: The transition to new interconnection technologies is most likely hindered by the generally smaller focus and efforts on multi-Si modules.

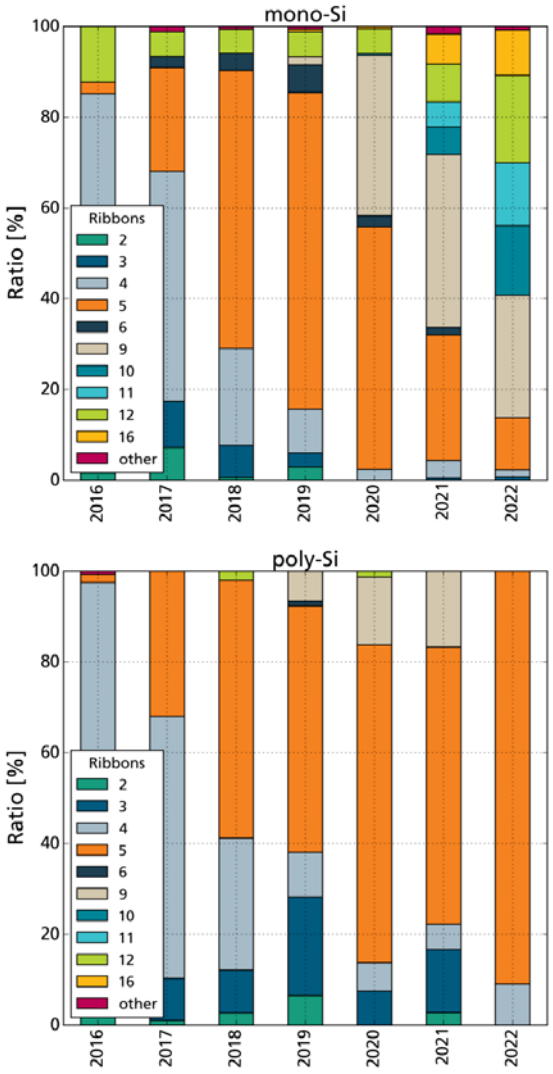


**Figure 2:** Share for different ribbon numbers per cell for mono-Si and poly-Si PV modules

The development of the module formats and cell count did not change for a longer period. The share of 60-cell and 72-cell modules was almost constant from 2012 until 2017 for mono-Si modules at 80 % (Figure 3). Other module layouts with typically less than 60 cells played a minor role. But since 2017, the dominating formats were steadily replaced by half-cell modules with 120 and 144 cells. The overall share of these full-cell and half-cell modules remains above 80 % until 2021. In the last months, many diversified module concepts with various cell counts and sizes arose.

For poly-Si modules, the classical layout with 60 and 72 full-cells is still dominating with more than 70 % to date. The share of the corresponding half-cell modules with 120 and 144 cells increased over the years. Other formats for poly-Si modules are barely relevant.

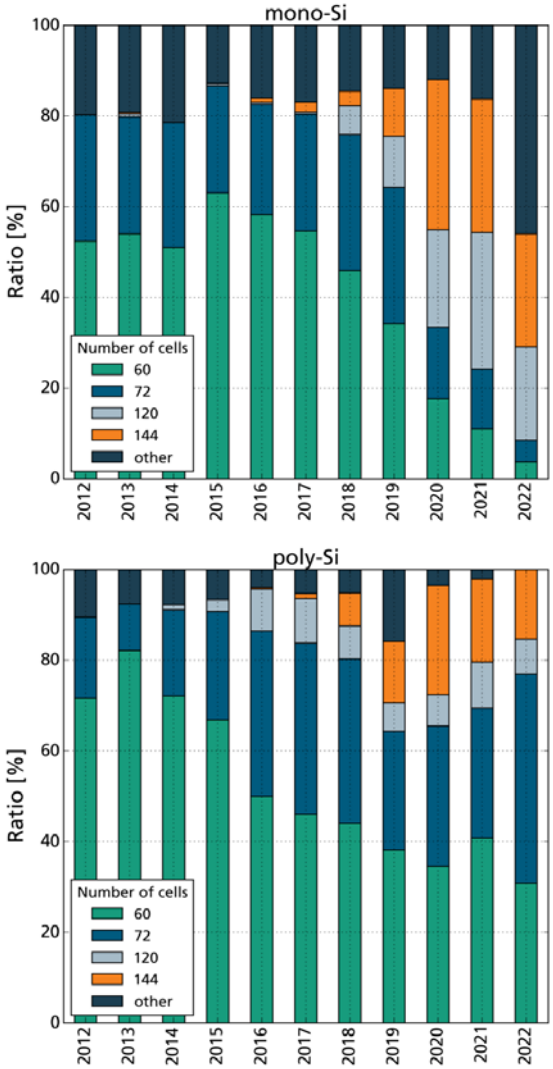


**Figure 3:** Share for modules with different number of cells for mono-Si and poly-Si PV modules

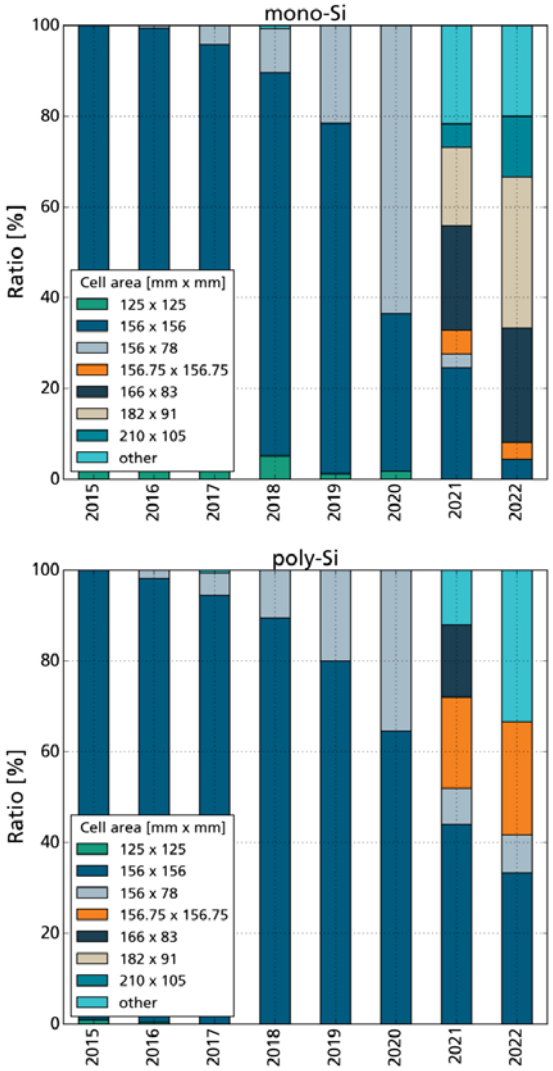


**Figure 4:** Share for cell dimensions for mono-Si and poly-Si PV modules

The cell sizes used in PV modules changed drastically in the last years (Figure 4). While for both, mono-Si and poly-Si PV modules, the standard cell size of 156 mm and 156.75 mm (M0 and M2 wafer) dominated with a share of about 80 % until 2019, the trend towards half-cut cells and larger wafer geometries changed the share. In 2020, the share of half-cut cells of 156 mm x 78 mm (M0/M2 wafer) raised and was in the following years replaced by half-cut cells of 166 mm x 83 mm (M6 wafer), 182 mm x 91 mm (M10 wafer) and 210 mm x 105 mm (M12 wafer) size.

For poly-Si modules, the full-cell formats of M0 wafers and M2 wafers (156.75 mm x 156.75 mm) still have a share greater 50 % to date.

The share of other cell formats is raising up to about 20 % share, but despite the larger diversity, none of the module types with e.g., M3 or M4 wafers or modules with third-cut cells have a significant share. So, all these formats are summarized in category “other”.

3.3 STC results

5358 STC measurements of mono-Si and poly-Si PV modules were filtered and analyzed. Mono-Si modules were divided in 2 subcategories: Silicon-Heterojunction (SHJ) and others, which is indicated by “not specified”. There is no differentiation between passivated emitter and rear cell (PERC), aluminum back surface field (Al BSF), TOPCon, MWT, IBC or other cell-technologies because the information was not available for most of the modules.

Figure 5 and Figure 6 show the development of module efficiency and fill factor (FF) over the last 10 years. The lines indicate the measured median for each category per year. The colored band indicates the efficiency interquartile range (IQR) from 25 % percentile to 75 % percentile, which represents 50 % of the results. The mono-Si modules improved almost constantly from 15 % in 2012 to 20 % in 2022, which is an efficiency improvement of 0.5 %-points per year. The efficiency of mono-Si SHJ Modules is even about 0.6 % higher over the last years.

The efficiency gain over the years for poly-Si modules is less than for mono-Si modules and converged at around 17 % since 2020. From 2012 to 2020, the efficiency gain was 0.3 %-points per year. A reason for the stagnation of

the efficiency could be the switch of manufacturers towards mono-Si modules and their higher potential towards higher efficiencies. Hence, the investments in the development of poly-Si modules were reduced. This is supported by the share of measured poly-Si PV module types which decreased drastically since 2018 whereas the number of mono-Si module types in the lab is constantly high.

FF increased from about 75 % in 2012 to almost 80 % in 2022 for mono-Si modules. The values are slightly higher for mono-Si SHJ modules. For poly-Si modules, FF remains below 78 % in the last years. The use of half-cut cells [8] is one example how the FF was improved in the last years.

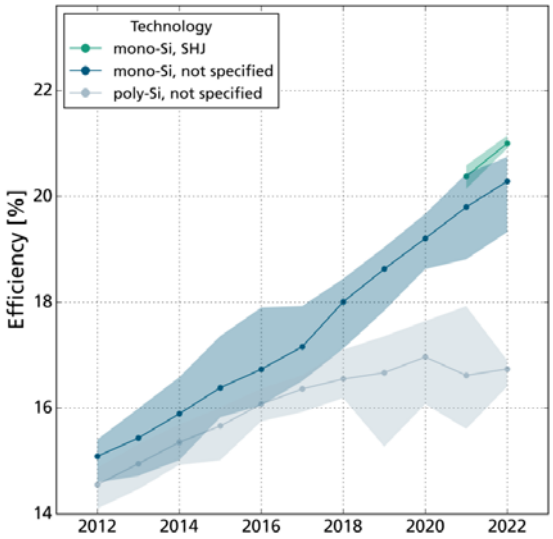


**Figure 5:** Development of the module efficiency over the last 10 years; the median and the interquartile range (IQR) are shown for mono-Si SHJ, mono-Si, and poly-Si modules

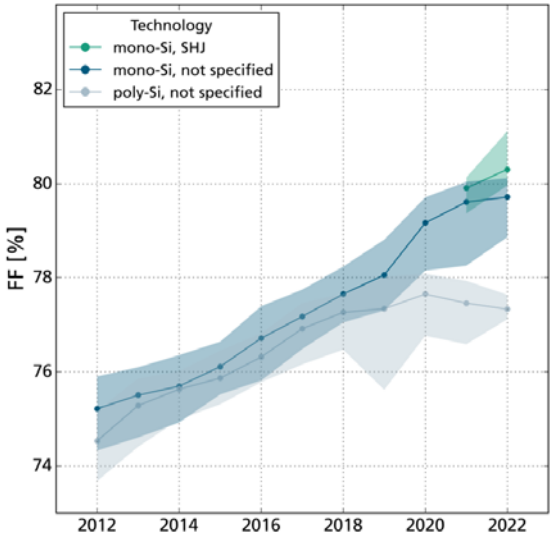


**Figure 6:** Development of the module FF over the last 10 years; the median and the interquartile range (IQR) are shown for mono-Si SHJ, mono-Si, and poly-Si modules

Figure 7 shows the $V_{OC}$ for mono-Si modules. A trend towards higher $V_{OC}$ is visible for all types. The cell interconnection of half-cell modules yields to the same $V_{OC}$ as for full-cell modules. Therefore, 60-cell and 120-cell modules respectively 72-cell and 144-cell modules have nearly the same $V_{OC}$. The gap between those two $V_{OC}$ levels can be explained by the difference of in-series connected cells, which define the module $V_{OC}$.

The larger fluctuations mainly of the 120-cell modules in the last years can be explained by the mixture of SHJ modules and other technologies in this graph. The SHJ technology yields higher $V_{OC}$ values about 44.5 V (742 mV per cell) compared to 41.3 V for other technologies (688 mV per cell) [9].

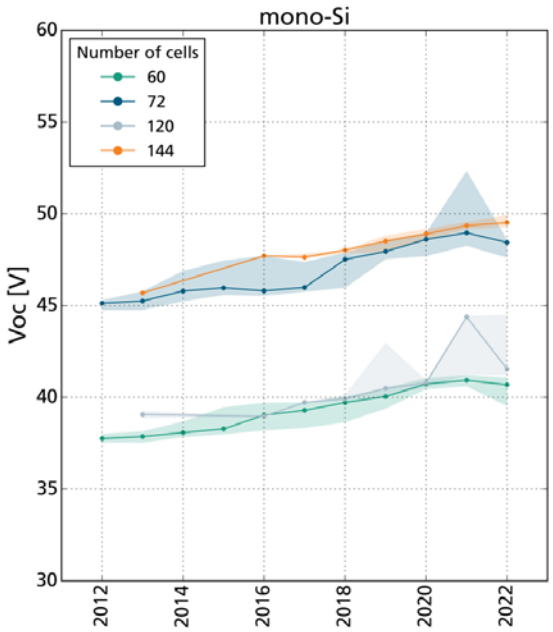


**Figure 7:** Development of the module open circuit voltage ($V_{OC}$) over the last 10 years; the median and the interquartile range (IQR) are shown for mono-Si modules with 60, 72, 120, and 144 cells

Beside the trends over time, it is interesting to filter the measured data by some module characteristics. In Figure 8, a boxplot shows the module efficiencies for different number of ribbons for mono-Si and poly-Si modules. The boxplot shows the median, the interquartile range (IQR), and the whiskers. The lower whisker limit Q1 - 1.5 * IQR and the upper whisker limit Q3 + 1.5 * IQR define a range of 99.3 % of the measured data.

With increasing number of ribbons, the module efficiency increases. This trend correlates with the efficiency over time as presented before because the cell design was developed over the years starting from 2-ribbon cells towards 9- or 10- ribbon cells respectively multiwire technology with more than 10 wires nowadays. Of course, the number of ribbons is not affecting the increase in efficiency directly. Larger cells as well as optimized cells yield to higher currents but resulting in increased electrical losses in the cell interconnections. Therefore, the optimization of the current distribution in the cell lead to more ribbons [4]. In addition, the underlying cell technology changed as well over time from BSF cells towards e.g., PERC cells and SHJ cells. Hence, the number of ribbons is not the cause for a gain in efficiency but

comes along with the cell improvement and the optimization of the module design e.g., by the cell-to-module analysis [10]. But the number of ribbons clearly indicates the development stage of the module respectively the cell technology.

The graph also shows that the diversity of used ribbons for poly-Si modules is less compared to mono-Si modules. The multiwire approach with 10 or more round wires did not occur for poly-Si modules.

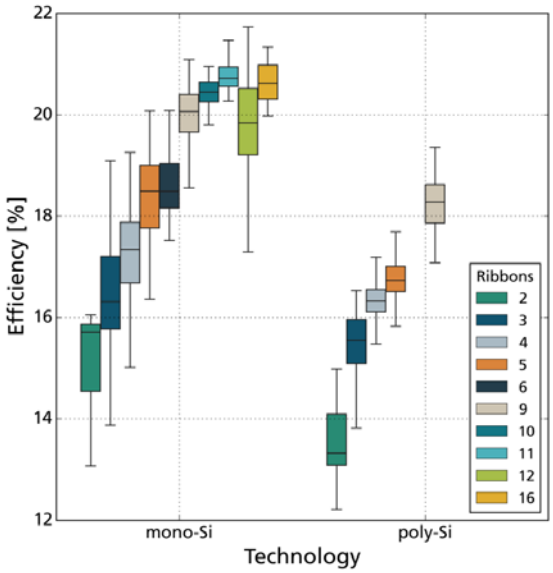


**Figure 8:** Boxplot of the module efficiency for mono-Si and poly-Si for different number of cell ribbons

In Figure 9, it is shown that modules with half-cut cells (120 and 144 cells) yield higher module efficiencies compared to full cell modules with 60 and 72 cells for both, mono-Si and poly-Si modules. The reason are the lower resistive losses in the module due to reduced internal currents per cell [8]. The large difference in the whisker size for full-cell mono-Si modules can be explained by the fact that full-cell modules were measured in 2012 and are still available in 2022. So, the efficiency gain over the years is summarized in the boxplot. Whereas half-cell modules entered the market about 5 years ago and where already higher efficiencies were state-of-the-art. Nevertheless, the potential for higher efficiencies for half-cell modules is also indicated by the upper whisker limit.

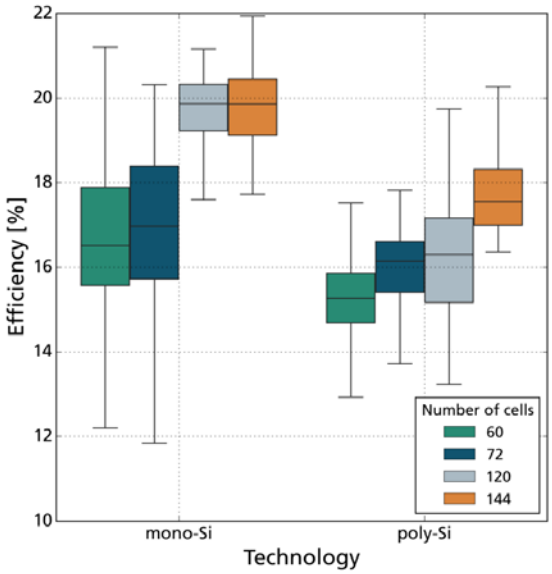


**Figure 9:** Boxplot of the module efficiency for mono-Si and poly-Si for different number of cells

3.4 Low light behavior

The trend of low light performance relative to STC over the years shows a negative development for mono-Si modules at first glance (Figure 11). However, as the comparison with the absolute efficiencies shows (Figure 10), the effect of generally higher efficiencies of modules from recent years clearly outweighs the low light behavior – meaning that newer modules, on average, outperform older modules despite seemingly worse low light behavior due to their absolute efficiency increase. This is important to consider when comparing PV module datasheets.

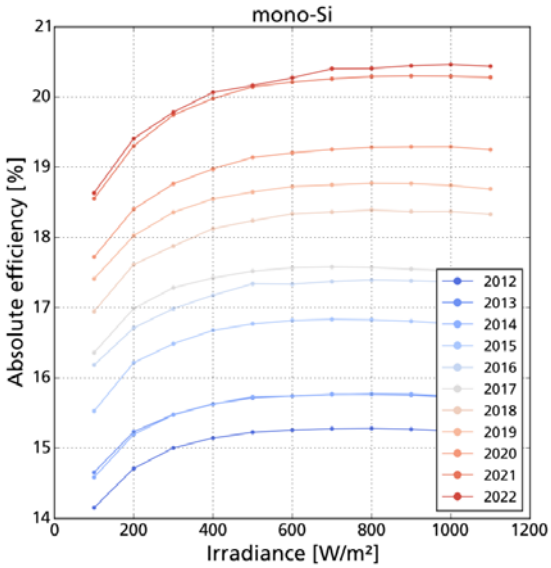


**Figure 10:** Yearly median of absolute efficiencies vs. irradiance for mono-Si modules

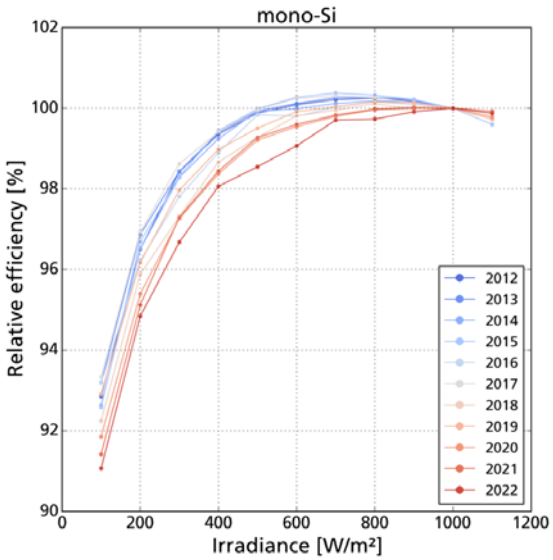


**Figure 11:** Yearly median of relative efficiencies vs. irradiance for mono-Si modules, normalized to the efficiency at STC

The absolute efficiencies for poly-Si modules are lower compared to mono-Si modules (Figure 12). However, the same negative trend for relative low light performance is visible (Figure 13).

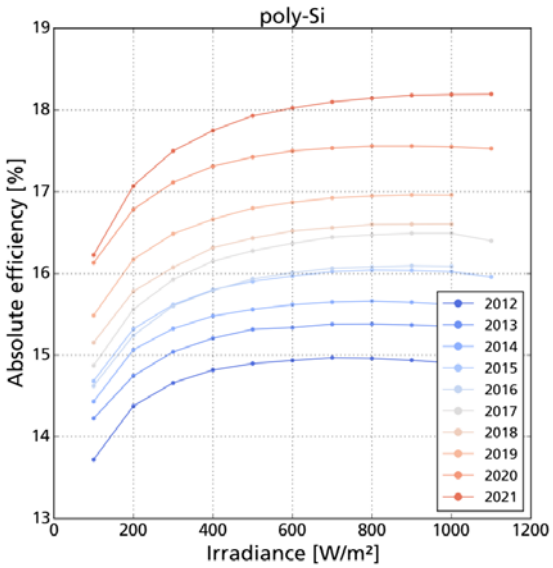


**Figure 12:** Yearly median of absolute efficiencies vs. irradiance for poly-Si modules

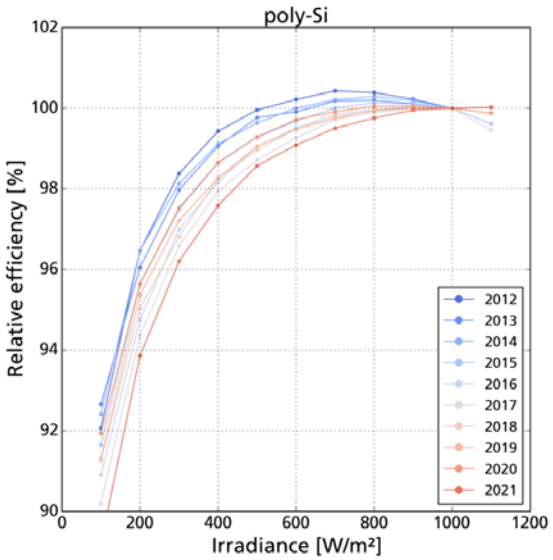


**Figure 13:** Yearly median of relative efficiencies vs. irradiance for poly-Si modules, normalized to the efficiency at STC

3.5 Temperature coefficient results

The temperature coefficient of power at maximum power point $TC_{Pmpp}$ (Figure 14) shows an absolute improvement over the years. This trend is most likely connected to the usage of newer cell technologies. Modules with SHJ cells, which appeared in the last years, have an even better performance than other mono-Si modules. 10 years ago, the poly-Si modules outperformed the $TC_{Pmpp}$ of mono-Si modules. This trend changed in 2017/18.

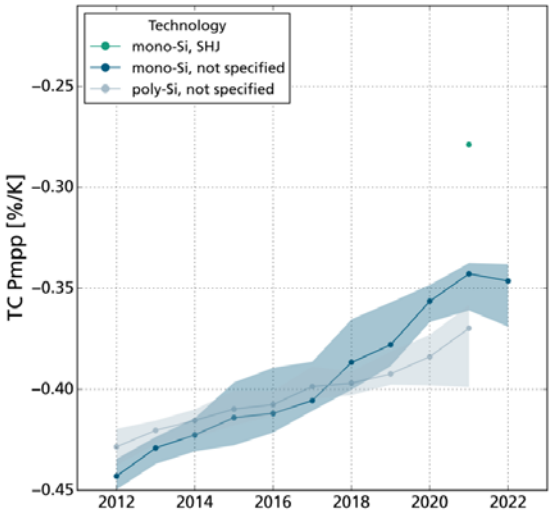


**Figure 14:** Development of the relative $TC_{Pmpp}$ over the last 10 years; the median and the interquartile range (IQR) are shown for mono-Si SHJ, mono-Si, and poly-Si modules

The temperature coefficient of the open-circuit voltage $TC_{Voc}$, which is also strongly related to the cell development [9], did also improve over the years for mono-Si modules. For poly-Si modules, an improvement is also visible but on a lower level. The SHJ modules outperform the other technologies with the highest $TC_{Voc}$.

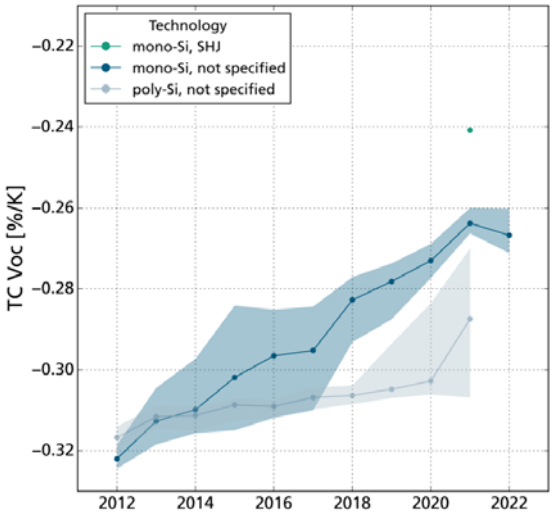


**Figure 15:** Development of the relative $TC_{Voc}$ over the last 10 years; the median and the interquartile range (IQR) are shown for mono-Si SHJ, mono-Si, and poly-Si modules

Temperature coefficients for short-circuit current $TC_{Isc}$ are very small and therefore the degree of uncertainty is normally higher than for the other temperature coefficients. Nevertheless, a clear distinction between mono-Si and poly-Si modules with higher coefficients is visible. It is noticeable, that from 2018/19, the trend towards higher coefficients was reversed.

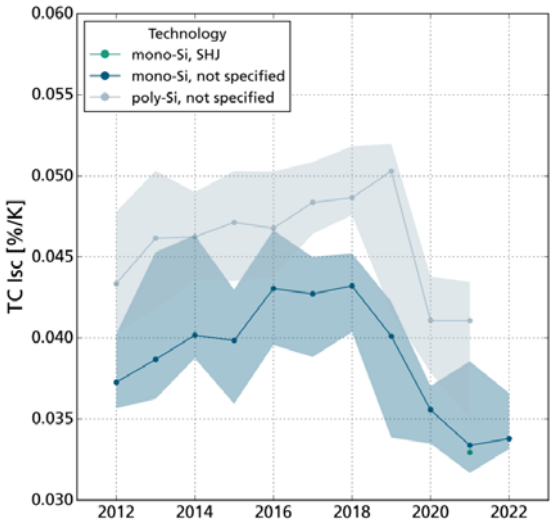


**Figure 16:** Development of the relative $TC_{Isc}$ over the last 10 years; the median and the interquartile range (IQR) are shown for mono-Si SHJ, mono-Si, and poly-Si modules.

## 4 CONCLUSION

In this work, we presented a methodology to make a large data set of measurements with high variability comparable. Multiple filters were applied to reduce the imbalance introduced by the variability of the data that was accumulated of our day-to-day business to convert it to a more expressive dataset. For STC, only 9.7 % of the data were available after filtering (40.9 % for G, and 58.1 % for TC). Nevertheless, the diversity of module types and producers in the filtered data set was maintained with 92.8 % (92.9 % for G, and 96.4 % for TC). Due to the large number of module types and producers in this evaluation, the shown graphs can therefore be interpreted as quite representative although all measurements were performed only in one laboratory which does certainly not cover the full market.

The data was analyzed to identify technological trends as far as client confidentiality allowed. Various technological trends were shown like the development from 2-ribbon cell interconnection towards 9-ribbon and multiwire interconnection replacing older technologies. The module layout with 60 or 72 full cells which was the standard for years, was successively replaced by half-cut cells with 120 and 144 cells per module. These modules represent the major share now. But increasing wafer formats and new module concepts are going to yield modules with wider variations in the number of cells in the upcoming years especially or mono-Si modules.

A constant increase of the absolute efficiencies even at low light conditions was shown for both, mono-Si and poly-Si modules. In contrast, the relative low light efficiencies decreased over time. This fact plays an important role e.g., in judgement and comparison of datasheets of different modules.

Along with the continuous development over cell level (from BSF to the introduction of passivation layers and SHJ), the TC for the modules improved. Modules with SHJ cells outperform other crystalline modules regarding the TC values.

We hope that the shown data and discussed trends can serve as reference, e.g., to evaluate if a module is state-of-the-art or fits to a certain year, to classify or rank module. Surely care must be taken with drawing general conclusions, especially regarding later trends of technical innovations. The fact that not all technological innovations could be resolved in this study and not all new trends reached the same grade of technical optimization must be considered. The study does not replace the individual characterization and evaluation of the module type of interest.

Furthermore, the data can be used as input for simulations to compare modules, e.g., CSER, which we plan to focus on in a follow-up publication.

In contrast to other publications on technological trends, such as the ITRPV roadmap [11], our work is not limited to mere estimations and opinions of the questionnaire participants but based on actual measurements and lessons learned from our daily lab work. Although inducing its own limitations (e. g. due to the large but still limited dataset) and remaining uncertainty about how representative our data is to the whole market, it still supplies a valuable resource from a different viewpoint to forecast future technology trends. We thus allow an alternative approach to support these considerations, because analyzing the speed and effects of technological changes that occurred in this industry's past can also educate assumptions on future developments.

## 5 ACKNOWLEGEMENTS

The authors of this work would like to thank all coworkers from Fraunhofer ISE's CalLab PV Modules, present and past, for performing the numerous measurements.

## 6 REFERENCES

References

[1] International Electrotechnical Commission (IEC). Photovoltaic devices – Part 1: Measurement of photovoltaic current-voltage characteristics. 3rd ed. (IEC 60904-1: 2020-09). Geneva, Switzerland: International Electrotechnical Commission (IEC); 2020.

[2] International Electrotechnical Commission (IEC). Photovoltaic devices – Procedures for temperature and irradiance corrections to measured I-V characteristics. 3rd ed. (IEC 60891: 2021-10). Geneva, Switzerland: International Electrotechnical Commission (IEC); 2021.

[3] International Electrotechnical Commission (IEC). Photovoltaic (PV) module performance testing and energy rating - Part 1: Irradiance and temperature performance measurements and power rating. 1st ed. (IEC 61853-1: 2011-01). Geneva, Switzerland: International Electrotechnical Commission (IEC); 2011.

[4] Tummalieh A, Pfreundt A, Mittag M. Trend Tracking of Efficiency and CTM Ratio of PV Modules. In: 37th EU PVSEC 2020; 2020.

[5] Fraunhofer Institute for Solar Energy Systems ISE. Fraunhofer ISE's CalLab PV Modules Improves Measurement Uncertainty to Record Value of 1.1 %. Freiburg, Germany; 2020.

[6] Fokuhl E, Philipp D, Mülhöfer G, Gebhardt P. LID and LETID evolution of PV modules during outdoor operation and indoor tests. EPJ Photovolt. 2021; 12: 9, DOI: 10.1051/epjpv/2021009.

[7] Walter J, Rendler LC, Ebert C, Kraft A, Eitner U. Solder joint stability study of wire-based interconnection compared to ribbon interconnection. Energy Procedia 2017; 124: 515–25, DOI: 10.1016/j.egypro.2017.09.288.

[8] Guo S, Singh JP, Peters IM, Aberle AG, Walsh TM. A Quantitative Analysis of Photovoltaic Modules Using Halved Cells. International Journal of Photoenergy 2013; 2013: 1–8, DOI: 10.1155/2013/739374.

[9] Steinkemper H, Geisemeyer I, Schubert MC, Warta W, Glunz SW. Temperature-dependent modeling of silicon solar cells—Eg, ni, recombination, and VOC. IEEE J. Photovolt. 2017; 7(2): 450–7, DOI: 10.1109/JPHOTOV.2017.2651822.

[10] Hädrich I, Eitner U, Wiese M, Wirth H. Unified methodology for determining CTM ratios: Systematic prediction of module power. Sol Energ Mat Sol C 2014; 131: 14–23, DOI: 10.1016/j.solmat.2014.06.025.

[11] ITRPV. International Technology Roadmap for Photovoltaic (ITRPV): 13th edition, 2021 Results; 2022.